

# Momentum spectroscopy of fragment ions of a multiply charged $N_2O$ molecule under impact of 10-keV electrons

Pragya Bhatt, Raj Singh, Namita Yadav, and R. Shanker\*

*Atomic Physics Laboratory, Department of Physics, Banaras Hindu University, Varanasi 221005, India*

(Received 20 August 2012; published 20 November 2012)

The dissociative ionization of a  $N_2O$  molecule is studied at an electron energy of 10 keV using the multiple-ion-coincidence imaging technique. The complete as well as the incomplete Coulomb explosion pathways for  $N_2O^{2+}$  and  $N_2O^{3+}$  ions are examined and identified. The precursor-specific relative partial ionization cross sections for resulting fragment ions are obtained. It is found that about 81.8% of single ionization, 17.8% of double ionization, and about 0.4% of triple ionization of the parent molecule contribute to the total fragment ion yield. Furthermore, the relative ionic fractions for ion-pair and ion-triple formation are also determined. The kinetic energy release distributions for different coincidence channels are obtained and compared with the available data at lower energies of electron and photon impacts and with that of high-energy ion impact. From the angular correlation studies of fragment ions, it is inferred that states with bent geometries are involved for most of the fragmentation channels of  $N_2O^{2+}$  and  $N_2O^{3+}$  ions. The concerted and/or sequential nature of the six dissociation pathways is also assigned. No other experimental or theoretical data exist in the literature to compare with the results obtained at the considered impact energy.

DOI: [10.1103/PhysRevA.86.052708](https://doi.org/10.1103/PhysRevA.86.052708)

PACS number(s): 34.80.Gs, 34.80.Ht

## I. INTRODUCTION

The study of physics and chemistry of multiply charged molecules is a rapidly expanding area, and the dissociation of such molecular species, in particular for atmospheric molecules, has attracted much attention in the past [1–4]. A number of studies have been devoted to the study of various atmospheric molecules such as CO, CO<sub>2</sub>, CS<sub>2</sub>, OCS, N<sub>2</sub>O, etc. [1–3]. However, the N<sub>2</sub>O molecule has gained comparatively less attention despite being a potent greenhouse gas [5] and an ozone-depleting catalyst in the stratosphere [6]. There are several studies available for the dissociative partial-ionization cross sections (PICSS) [7,8] and for the dissociation dynamics of N<sub>2</sub>O [9–18]. Theoretical studies for the potential energy surfaces of multiply ionized precursors are scarce due to the complexity involved in such calculations [9,19]. However, the excited states of a multiply ionized molecule can be approached experimentally by measuring the kinetic energy release (KER) during the explosion of that precursor molecular ion. The experimentally observed KER is simply the sum of kinetic energies of all the constituent fragment ions detected for a particular dissociation pathway. The multiply ionized molecular species are generally produced by photon and charged-particle impacts which eventually explode due to the excess positive charges on the parent ion. The resulting collision fragments may or may not be internally excited. If the fragments are formed in their respective ground electronic states, the measured KER above the thermodynamic threshold for a given fragmentation channel will provide a particular electronic state of the precursor molecular ion. A few theoretical calculations for the dicationic states of N<sub>2</sub>O are available in the literature [9,19]; however, the triply and multiply ionized states of this molecule are not theoretically addressed so far. Price *et al.* [9] experimentally measured the

dicationic states of N<sub>2</sub>O by using photoionization and double-charge-transfer spectroscopy; they made use of theoretical calculations to identify these states. The Auger electron fragment-ion-coincidence experiments performed by Murphy and Eberhardt further elucidated the nature of the dicationic states of N<sub>2</sub>O [20]. Eland and Murphy [10] used the excitation source of low- and high-energy radiation and obtained the low-lying states of N<sub>2</sub>O<sup>2+</sup>. Few recent experimental data are also available for the KER of different fragmentation channels for multiply ionized N<sub>2</sub>O under electron, ion, and photon impacts [7,15–18]. In high-energy electron collision experiments such as of the present case, a wide range of excited states of the molecule may be accessed rather than the site and wavelength selective excitation as obtained in photoionization [10,12,21]. The molecular ion may also undergo geometrical deformation in such collision experiments besides the elongation of the equilibrium bond lengths [14,16]. To investigate the occurrence of such deformations under keV electron impact, we have measured the bond angle of the dissociating N<sub>2</sub>O<sup>3+</sup> ion.

In the present measurements, the technique of multiple-ion coincidence along with the information of position encoding is used for 10-keV electron interactions with N<sub>2</sub>O. The momentum vectors of the fragment ions generated in collision events are used to find the angular correlations of the departing fragments and the KER for a given dissociation channel. The mechanisms of dissociation for different channels are also explored and discussed. The precursor-specific relative PICSSs for the six fragment ions are obtained and used to determine the contribution of single, double, and triple ionization of N<sub>2</sub>O to the total fragment ion yield.

## II. EXPERIMENTAL METHOD AND DATA ANALYSIS

The details of the experimental setup and those of data analysis are given in our previous publications [22–24]. Briefly, a monoenergetic beam of electrons is made to collide

\*shankerorama@gmail.com

with a well-collimated  $N_2O$  (purity 99.99%, Matheson, Inc.) gas jet using a hypodermic needle. A single-stage Wiley McLaren-type time-of-flight (TOF) spectrometer [25] is used in the present experiment. The electron beam, the gas jet, and the axis of TOF spectrometer are aligned mutually perpendicular to each other. The reaction products are extracted by applying a homogeneous electric field of 119 V/cm; positive ions resulting from collision events are detected by a dual microchannel plate (MCP) mounted in one direction and ejected electrons are detected by a channeltron placed in the opposite direction. The electron signal is used to provide a reference to the arrival times for ions. Neutrals produced in the collision reactions are not detected. A delay line anode placed behind the MCPs is used to obtain the position information of the ions on the MCP. The TOF and position coordinates of the ions are used to calculate their corresponding momentum vectors [22]. The TOF spectrum of the produced ions following direct and dissociative ionization of the  $N_2O$  molecule by impact of 10-keV electrons has been recorded and studied earlier by us [8]. A typical ion-ion coincidence spectrum (raw data) resulting from the collisions of 10-keV electrons with  $N_2O$  is displayed in Fig. 1; the resulting fragmentation channels are labeled in the figure. The island labeled as C arises due to the random coincidence of the fragment ions with a periodic noise of about 5 MHz from some unknown external source which could not be removed during the data acquisition. Fortunately, it did not overlap with any true coincidence islands analyzed in the present study. This noise was also present in our previous measurements for  $CO_2$ , and one of the random coincidence islands generated due to this noise was found to overlap with the true island of  $O^+ + CO^+$  [24]. However, such random coincidences in addition to any other random coincidences if present in the complete Coulomb explosion (CE) channel ( $O^+ + CO^+$ ) were taken care of by considering only those events which satisfy the criteria of conservation of

momentum [24]. Similarly in the present study, the momentum of center of mass of the precursor ion is used to eliminate the random coincidences from the complete CE channels (e.g.,  $N^+ + NO^+$ ,  $N^+ + N^+ + O^+$ , etc.). For incomplete CE channels (e.g.,  $N^+ + N^+ + O$  and  $N^+ + O^+ + N$ ), a method described in Ref. [26] has been used for subtraction of random coincidences; for a  $N^+ + N^+ + O$  channel, an additional correction is made for the spurious signals coming due to the triple-ion-coincidence channel  $N^+ + N^+ + O^+$ . The correction in counts for  $N^+ + NO^+$ ,  $O^+ + N_2^+$ ,  $N^+ + O^+ + N$ ,  $N^{2+} + NO^+$ , and  $N^+ + N^+ + O^+$  channels is on average about 7%; however, a maximum random coincidence correction of 38% is made in the case of a  $N^+ + N^+ + O$  channel.

The corrected coincidence counts for double- and triple-ion coincidence channels are further corrected for the detection efficiency ( $D = 0.24$ ) of the employed TOF spectrometer in order to put them on the same scale (see Ref. [23]). These corrected counts are used to calculate the relative ionic fractions (RIFs) of different double- and triple-ion coincidence channels. For obtaining the precursor-specific PICSSs of fragment ions, the counts observed in single-ion coincidence spectrum with a total charge of one ( $N^+$ ,  $O^+$ ,  $N_2^+$ , and  $NO^+$ ) are treated as events arising only from  $N_2O^+$ ; similarly, the counts observed in single- to triple-ion coincidence spectra with a total charge of two ( $N^{2+}$ ,  $O^{2+}$ ,  $N^+ + NO^+$ ,  $O^+ + N_2^+$ ,  $N^+ + N^+ + O$ , and  $N^+ + O^+ + N$ ) and three ( $N^{2+} + NO^+$  and  $N^+ + N^+ + O^+$ ) are treated as events arising only from  $N_2O^{2+}$  and  $N_2O^{3+}$ , respectively. These cross-section values are put on a relative scale by dividing them with the corrected counts of  $N_2O^+$ .

The momentum vectors of individual ions associated with a particular dissociation channel are used to calculate their respective KEs; the sum of KEs of these ions equals the KER for a given fragmentation channel. The angular correlations among the fragments are obtained by calculating the free angle  $\alpha$  between the two ions [24].

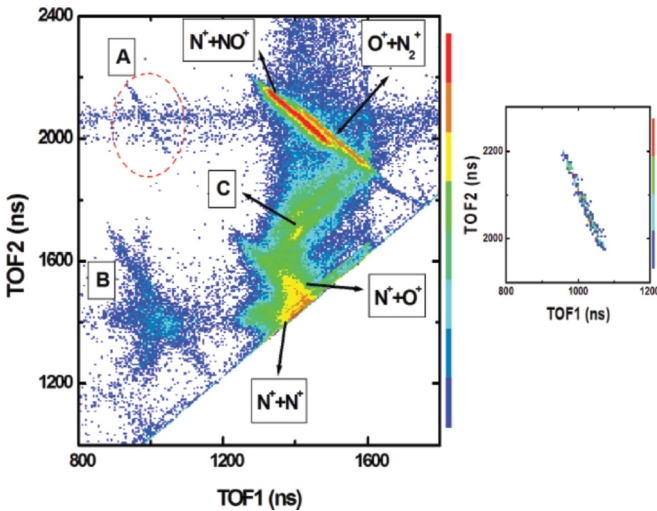


FIG. 1. (Color online) Ion-ion coincidence map (raw data) for 10-keV electron interactions with  $N_2O$ . Inset on the right side shows the background subtracted data for the island A appearing due to the coincidence channel  $N^{2+} + NO^+$ . The island B is appearing due to the overlap of three coincidence channels  $N^{2+} + N^+$ ,  $N^{2+} + O^+$ , and  $O^{2+} + N^+$ . The island C is due to inherent random coincidences (see text).

### III. RESULTS AND DISCUSSION

#### A. Relative ionic fractions and precursor-specific relative partial ionization cross sections

We have identified nine coincidence channels for the dissociation of  $N_2O^{q+}$  ( $q = 2, 3$ ) viz.  $N^+ + NO^+$ ,  $O^+ + N_2^+$ ,  $N^+ + N^+ + O$ ,  $N^+ + O^+ + N$ ,  $N^+ + N^+ + O^+$ ,  $N^{2+} + NO^+$ ,  $N^{2+} + N^+ + O$ ,  $N^{2+} + O^+ + N$ , and  $O^{2+} + N^+ + N$  (see Fig. 1); the last three channels are not analyzed due to their low counting statistics and their overlaps among themselves. Using the corrected counts for these channels as discussed above in Sec. II, the RIFs are obtained and presented in Table I;  $N^+ + NO^+$  is found to be the most dominant channel. For comparing the abundances of different channels with the corresponding abundances from a theoretical model [19] and with those of few experimental data from the literature [9, 15–17], only two dominant channels,  $N^+ + NO^+$  and  $O^+ + N_2^+$ , are considered. It is found that these two channels are formed in the ratio of 2.9:1, which is in good agreement with the *ab initio* calculations of Lévassieur and Millié [19] and with the experimental results obtained from photon impact [9, 17] and intense laser fields [16]; however, the abundances of

TABLE I. Comparison of the relative ionic fractions of different coincidence channels observed in 10-keV electron interactions with  $N_2O$  with the earlier reported experimental results and a theoretical model. Errors (%) are given in parentheses.

Coincidence channel	RIFs (%)					Theoretical prediction <sup>e</sup>
	Present	Experimental results				
		24–100 nm photons <sup>a</sup>	800 nm intense laser <sup>b</sup>	40 eV photons <sup>c</sup>	5.9 MeV/u $Xe^{43+}$ ions <sup>d</sup>	
$N^+ + NO^+$	60.2 (<1)	77.9	74.4	75	59	75
$O^+ + N_2^+$	21.2 (<1)	20.8	24.2	25	41	25
$N^+ + N^+ + O$	2.4(4)					
$N^+ + O^+ + N$	14.6(7)	1.3				
$N^+ + N^+ + O^+$	1.5(2)		1.4			
$N^{2+} + NO^+$	0.2(6)					

<sup>a</sup>Reference [9].

<sup>b</sup>Reference [16].

<sup>c</sup>Reference [17].

<sup>d</sup>Reference [15].

<sup>e</sup>Reference [19].

these two channels were found to be of comparable magnitudes under 5.9 MeV/u  $Xe^{43+}$  ion impact [15] (see Table I). In addition to the dominant contribution of the above-mentioned complete CE channels, the contributions from the incomplete CE channels ( $N^+ + N^+ + O$  and  $N^+ + O^+ + N$ ) in our experiment are much more significant as compared to the contribution reported by an earlier measurement [9]; a likely reason for such an observation is the relatively high energy of impact used in the present case which may populate more highly excited states of the precursor ion.

The precursor-specific relative PICSs  $\sigma_n$  ( $n = 1-3$ ) for the fragment ions ( $NO^+$ ,  $N_2^+$ ,  $O^+$ ,  $N^+$ ,  $N^{2+}$ , and  $O^{2+}$ ) are presented in Table II; a combined value for the cross sections of  $N^{2+}$  and  $O^{2+}$  ions are reported since their peaks are not resolved in the TOF spectrum [8]. The values  $\sigma_1$ ,  $\sigma_2$ , and  $\sigma_3$  provide the contributions from singly, doubly, and triply ionized  $N_2O$  to a particular fragment ion yield, respectively. The sum of individual contributions  $\sum \sigma_n$  (last column of Table II) for a particular fragment ion from these three ionization events yields the relative PICS for that ion. The relative PICSs of fragment ions of  $N_2O$  obtained by this method are in a good agreement with our recent measurements [8]. We further estimate that about 81.8% of single ionization, 17.8% of double ionization, and about 0.4% of triple ionization of the parent  $N_2O$  molecule contribute to the total fragment ion yield. Thus, the multiple ionization of  $N_2O$  makes a significant

TABLE II. Precursor-specific partial ionization cross sections,  $\sigma_n$  ( $n = 1-3$ ), for fragment ions formed in collisions of 10-keV electrons with  $N_2O$  expressed relative to the cross section for formation of  $N_2O^+$ . The suffix  $n$  denotes the ionization state of  $N_2O$  after the removal of  $n$  number of electrons.

Ion species	$\sigma_1$	$\sigma_2$	$\sigma_3$	PICS = $\sum \sigma_n$
$NO^+$	0.510	0.061	0.0002	0.570
$N_2^+$	0.155	0.021		0.176
$O^+$	0.085	0.036	0.0015	0.123
$N^+$	0.224	0.080	0.0031	0.307
$N^{2+}, O^{2+}$		0.014	0.0002	0.014

contribution of about 18% to the total fragment ion yield at the present energy of impact.

## B. Dynamics and mechanisms of dissociation

### 1. Complete Coulomb explosion channels

(a)  $N^+ + NO^+$ . This is a simple two-body dissociation channel in which the two fragment ions are found to fly back to back with equal momenta after dissociation of the precursor  $N_2O^{2+}$  ion. The slope of the corresponding island is  $-45^\circ \pm 1^\circ$ , as clearly seen in the ion-ion coincidence map (see Fig. 1).

The KER distribution for this channel is shown in Fig. 2. To model the KER distribution for this channel correctly, two peaks are fitted at  $4.0 \pm 0.5$  and  $5.3 \pm 0.6$  eV with weightings of 58:42, as given in Table III. The CE model predicts a much higher value of KER (12.7 eV) due to the assumption of localized point charges at equilibrium bond

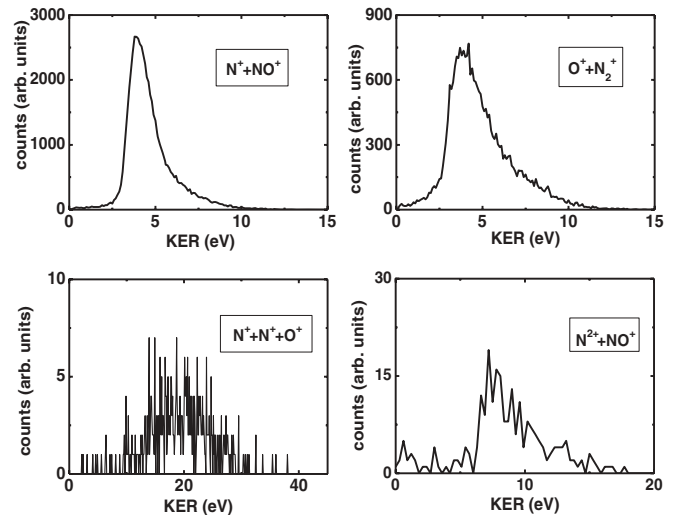


FIG. 2. KER distributions for the complete Coulomb explosion channels observed in the dissociation of  $N_2O^{2+}$  (upper panel) and  $N_2O^{3+}$  (lower panel) in 10-keV electron impact with  $N_2O$ .

TABLE III. Comparison of kinetic energy release in different dissociation channels obtained by impact of 10-keV electrons on  $N_2O$  with the earlier reported experimental results.

Coincidence channel	KER (eV)							
	Electron impact			Photon impact		Intense laser field		Ion impact
	Present	50 eV <sup>a</sup>	1300 eV <sup>b</sup>	25.6 nm <sup>b</sup>	24–100 nm <sup>c</sup>	795 nm (5 PW/cm <sup>2</sup> ) <sup>d</sup>	800 nm (0.16 PW/cm <sup>2</sup> ) <sup>e</sup>	5.9 MeV/u Xe <sup>43+</sup> ions <sup>f</sup>
$N^+ + NO^+$	4.0 ± 0.5 5.3 ± 0.6	6.3 ± 1.0	7.2 ± 0.7	7.2 ± 0.4	6.3 ± 0.3	6.5 ± 2.0	6.8 ± 2.0	7.0
$O^+ + N_2^+$	3.5 ± 0.4 4.4 ± 0.5 5.6 ± 0.7	3.2 ± 1.0 5.8 ± 1.0 9.0 ± 1.0	7.5 ± 1.5	7.4 ± 1.0	3.2 5.8 8.5	5.6	6.2 ± 1.0	5.0 6.5
$N^{2+} + NO^+$	8.4 ± 1.0		17.5 ± 3.0			11.9 ± 2.0		
$N^+ + N^+ + O$	4.7 ± 0.5 7.8 ± 0.9 13.0 ± 2.0	5.0 ± 1.0 <sup>g</sup> 8.0 ± 1.0 <sup>g</sup>						
$N^+ + O^+ + N$	3.6 ± 0.4 7.5 ± 0.9 13.4 ± 3.0	5.0 ± 1.0 7.0 ± 1.0	9.5 + 12.5	5.2 ± 1.0	4.7 ± 1.0			
$N^+ + N^+ + O^+$	19.0 ± 2.2		30.3 ± 3.0					

<sup>a</sup>Reference [7].<sup>b</sup>Reference [10].<sup>c</sup>Reference [9].<sup>d</sup>Reference [14].<sup>e</sup>Reference [16].<sup>f</sup>Reference [15].<sup>g</sup>At 65-eV electron energy.

lengths. This model is, however, found quite reliable in cases where the degree of ionization of the molecule is high [27]. The present KER values underestimate the KERs available in the literature [7,9,10,14–16] (see Table III). The KER values above the thermodynamic threshold for this channel (28.7 eV) give the excited-state energies of the precursor  $N_2O^{2+}$  to be 32.7 and 34.0 eV; these are much lower than the range of energies for vertical Franck-Condon transitions (34.5–36.0 eV) as obtained by photoionization experiments [9]. If we consider  $NO^+$  to be formed in its ground electronic state with a maximum accessible vibrational energy of 1 eV [9], the energy of the excited precursor would be  $33.7 \pm 0.5$  and  $35.0 \pm 0.6$  eV; the latter value lies well within the vertical Franck-Condon transition energies as given above. However, in the former case, either the dissociation products are formed in their excited states in contrast to the earlier observations [9] or the dicationic states lying outside the Franck-Condon region are populated by indirect double ionization processes [13,28]. The good agreement of the RIFs of  $N^+ + NO^+$  and  $O^+ + N_2^+$  channels, as discussed in Sec. III A above, with the theoretical calculations [19] made for their respective ground states rules out the possibility that the fragments are formed in their excited states. Therefore, indirect ionization processes are the most likely path to play a crucial role at the present impact energy for a precursor state at 32.7 eV.

(b)  $O^+ + N_2^+$ . This is also a two-body dissociation channel showing a sharp narrow island with a slope of  $-45^\circ \pm 1^\circ$  in the coincidence map shown in Fig. 1. The KERs obtained for this channel are  $3.5 \pm 0.4$ ,  $4.4 \pm 0.5$ , and  $5.6 \pm 0.7$  eV with weightings 18:30:52 (see Fig. 2 and Table III). The experimental KERs for this channel are again much smaller than

the prediction of CE model (12.1 eV) and the earlier reported measurements [7,9,10,14–16] (see Table III). However, the KER at 3.5 eV does show a good agreement with the data of Love and Price [7] and Price *et al.* [9]. Similarly, the KER at 5.6 eV shows a good agreement with the data of Love and Price [7], Price *et al.* [9], and Hishikawa *et al.* [14]. The possible excited-state energies for this channel above its thermodynamic threshold (30.9 eV) are  $34.4 \pm 0.4$ ,  $35.3 \pm 0.5$ , and  $36.5 \pm 0.7$  eV. Out of these three values, only 34.4 eV lies outside the range of most probable threshold energies within the Franck-Condon zone (35.0–36.5 eV) [9]. If we consider the maximum vibrational energy accessible to  $N_2^+$  as 0.2 eV [9], the excited state with energy of  $34.6 \pm 0.4$  eV would also lie in the Franck-Condon region. Thus, for the present case we conclude that both the fragments are formed in their ground states, which is also confirmed by the agreement of RIFs with the theoretical prediction [19], as discussed above in Sec. III A. However, the contribution of indirect ionization processes may not be completely ruled out for the lowest KER for this channel, which shows marginal agreement with the Franck-Condon region. In fact, in the double-photoionization spectrum of  $N_2O$ , the lines well below the molecular double-ionization potential around 34.5–35.3 eV have been observed due to the fragment autoionization [28].

(c)  $N^{2+} + NO^+$ . This is again a two-body dissociation channel appearing as a relatively less intense island in the ion-ion coincidence map (see Fig. 1, inset on right side) with a slope of  $-64^\circ \pm 1^\circ$ . The KER distribution for this channel is shown in Fig. 2; and the KER for this channel is  $8.4 \pm 1.0$  eV, which is lower than the earlier reported data [10,14] (see Table III). The indirect ionization processes must play a

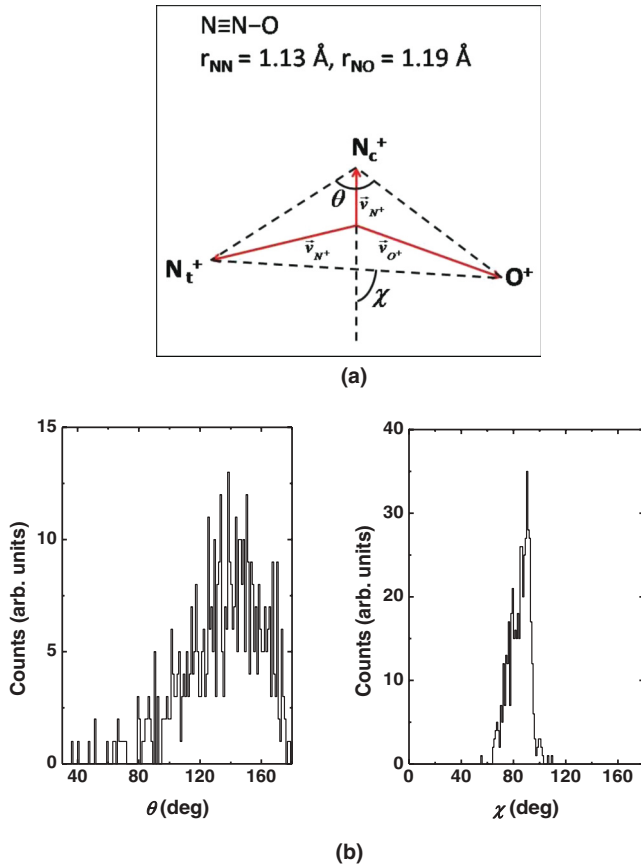


FIG. 3. (Color online) (a) Definition of angles  $\theta$  and  $\chi$  in velocity space.  $r_{\text{NN}}$  and  $r_{\text{NO}}$  are the equilibrium bond lengths of the  $\text{N}_2\text{O}$  molecule.  $\text{N}_c^+$  and  $\text{N}_t^+$  are the central and terminal nitrogen fragment ions, respectively.  $\vec{v}$  represents the velocity vector of an ion. (b) The distribution of N-N-O bond angle  $\theta$  (left) and the distribution of angle  $\chi$  (right) as observed in a  $\text{N}^+ + \text{N}^+ + \text{O}^+$  fragmentation channel of  $\text{N}_2\text{O}^{3+}$  for 10-keV electron impact with  $\text{N}_2\text{O}$ .

vital role in the formation of the triply charged precursor of  $\text{N}_2\text{O}$  which gives rise to the present value of KER.

(d)  $\text{N}^+ + \text{N}^+ + \text{O}^+$ . This is a three-body complete Coulomb explosion channel. The KER for this channel is  $19.0 \pm 2.2$  eV (see Fig. 2 and Table III); this value clearly underestimates the value predicted by the CE model (31 eV) due to the reasons as described above. No theoretical predictions are available for the potential energy surfaces of the corresponding  $\text{N}_2\text{O}^{3+}$  precursor ion.

To deduce the geometry of the precursor trication ( $\text{N}_2\text{O}^{3+}$ ) dissociating into the  $\text{N}^+ + \text{N}^+ + \text{O}^+$  fragmentation channel, we have measured its bond angle  $\theta$  as defined in Fig. 3(a). The distribution of this angle is shown in Fig. 3(b), which shows that a large number of bent geometrical states of  $\text{N}_2\text{O}^{3+}$  are involved with a mean value of  $\theta = 140^\circ$ . This suggests that the  $\text{N}_2\text{O}$  molecule undergoes geometrical deformation in its triply ionized state. Previous works on  $\text{N}_2\text{O}$  also suggested a similar type of geometrical deformation of  $\text{N}_2\text{O}^{3+}$ , with  $\theta$  decreasing from  $170^\circ$  to  $100^\circ$  along with elongation of the NN and NO distances from 1.43 to 1.67 times more than their equilibrium values under intense laser fields [16].

In order to explore the dissociation mechanisms for this channel, the parameter  $\chi$  as defined in Fig. 3(a) is utilized.

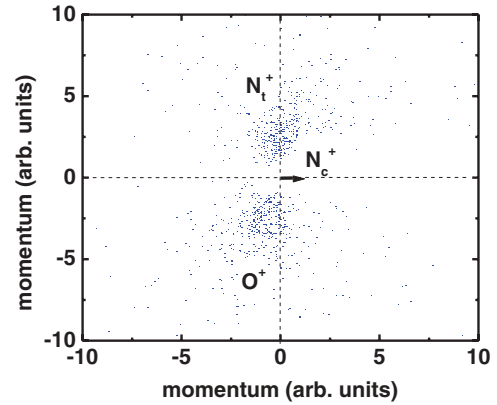


FIG. 4. (Color online) Newton diagram for complete Coulomb explosion channel  $\text{N}_t^+ + \text{N}_c^+ + \text{O}^+$  originated from the dissociation of  $\text{N}_2\text{O}^{3+}$  in 10-keV electron impact with  $\text{N}_2\text{O}$ . The momentum vector of central nitrogen ion  $\text{N}_c^+$  is taken along the  $x$  axis as reference, and the relative momentum vectors of the  $\text{N}_t^+$  and  $\text{O}^+$  ions are plotted in the upper and lower half, respectively.

For a triply ionized symmetric molecule  $\text{AB}_2$ , if both the A-B bonds break simultaneously, leaving the central A ion at rest, a strong angular correlation will result in a  $\chi$  value of  $90^\circ$ , showing the concerted dissociation. In fact, we do observe such correlation for  $\chi$  in the case of  $\text{N}_2\text{O}^{3+}$  but not at  $90^\circ$ , rather, at a slightly lower angle around  $86^\circ$  [see Fig. 3(b)]. This is mostly expected due to the asymmetric mass distribution in  $\text{N}_2\text{O}$  due to which the momentum of the terminal nitrogen ( $\text{N}_t$ ) ion and that of the oxygen ion are found to be slightly different, allowing the central nitrogen ( $\text{N}_c$ ) ion to gain some finite momentum as per the law of conservation of momentum. To visualize this, the Newton diagram for this channel is also plotted and shown in Fig. 4, which shows that most of the  $\text{N}_t^+$  and  $\text{O}^+$  ions are emitted at  $90^\circ$  and  $106^\circ$ , respectively, relative to the  $\text{N}_c^+$  ion, referring to the concerted dissociation process.

## 2. Incomplete Coulomb explosion channels

(a)  $\text{N}^+ + \text{N}^+ + \text{O}$ . The slope and shape of this island appearing in Fig. 1 could not be ascertained due to its low counting statistics. The KERs ( $4.7 \pm 0.5$ ,  $7.8 \pm 0.9$ , and  $13.0 \pm 2.0$  eV) for this channel are given in Table III, along with the earlier data reported at very low electron impact energy of 65 eV [7]; the distribution of KER is shown in Fig. 5. These KER values above the thermodynamic threshold for this channel (40.6 eV) provide the excited-state energies of  $\text{N}_2\text{O}^{2+}$  as  $45.3 \pm 0.5$ ,  $48.4 \pm 0.9$ , and  $53.6 \pm 2.0$ ; the former two values are in good agreement with the data of Love and Price [7].

The Newton diagram for this channel is shown in Fig. 6, with the first arriving  $\text{N}^+$  ion (termed as fast  $\text{N}^+$  ion) as reference along the  $x$  axis. From the most intense distribution in this figure, it can be found that both the slow  $\text{N}^+$  ion and the neutral O atom are moving away from the fast  $\text{N}^+$  ion at about  $116^\circ$  and  $162^\circ$ , respectively, indicating the two-step dissociation of the precursor  $\text{N}_2\text{O}^{2+}$ . In the first step the  $\text{N}_2\text{O}^{2+}$  molecular ion dissociates into  $\text{N}^+$  and  $\text{NO}^+$  ions and after that the  $\text{NO}^+$ , which is moving to the left, breaks into  $\text{N}^+$  and  $\text{O}$ .

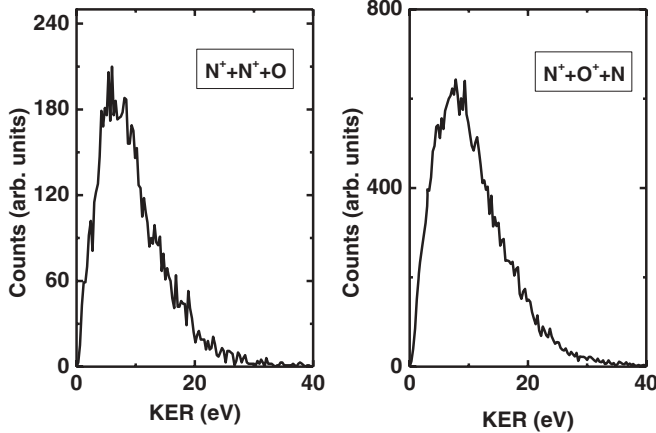


FIG. 5. Same as in Fig. 2 but for incomplete Coulomb explosion channels observed in the dissociation of  $N_2O^{2+}$ .

Thus, this dissociation channel follows the steps:  $N_2O^{2+} \rightarrow N^+ + NO^+ \rightarrow N^+ + N^+ + O$ .

(b)  $N^+ + O^+ + N$ . This is the most dominant channel among the incomplete CE channels as observed in Fig. 1. The slope of the most intense central part of this island is found to be about  $-48^\circ \pm 3^\circ$ ; however, it is difficult to judge the shape of the island correctly. The slope of this island suggests the presence of a concerted dissociation of the precursor molecular ion for which the slope should be  $-45^\circ$ . The slight mismatch of the value of slope from  $-45^\circ$  shows that there may be a contribution from the sequential dissociation of  $N_2O^{2+}$ . Furthermore, the slope of this island may be different for its less intense outward expansion than its most intense central part, which will lead to an additional dissociation mechanism; these are not distinguishable in our coincidence map (see Fig. 1). A detailed description of the mechanisms of dissociation based on the slope of this island produced by photoionization is given in Ref. [10]. The Newton diagram for this channel is shown in Fig. 7. The figure shows

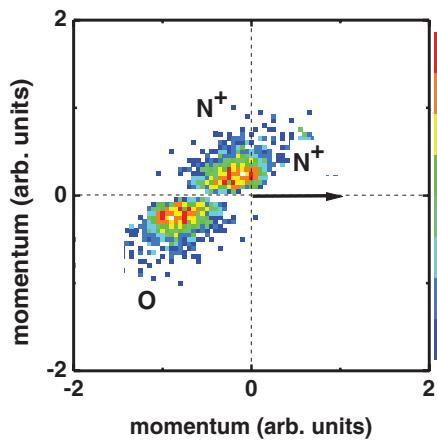


FIG. 6. (Color online) Newton diagram for incomplete Coulomb fragmentation channel  $N^+ + N^+ + O$  originating from the dissociation of  $N_2O^{2+}$  in 10-keV electron impact with  $N_2O$ . The momentum vector of fast  $N^+$  ions is taken along the  $x$  axis as reference and the relative momentum vectors of the slow  $N^+$  ion and neutral  $O$  atom are plotted in the upper and lower half, respectively.

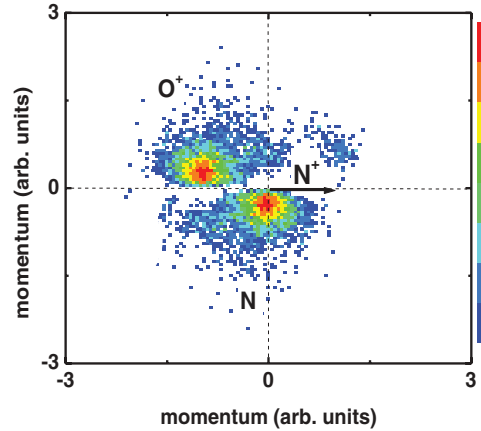


FIG. 7. (Color online) Same as in Fig. 6 but for  $N^+ + O^+ + N$ . The momentum vector of the  $N^+$  ion is taken along the  $x$  axis as reference and the relative momentum vectors of the slow  $O^+$  ion and neutral  $N$  atom are plotted in the upper and lower half, respectively.

that the momentum vectors of most of the  $O^+$  ions and the neutral  $N$  atoms with respect to the momentum vector of  $N^+$  (plotted along the  $x$  axis) are distributed around  $164^\circ$  and  $90^\circ$ , respectively, giving rise to the sequential decay of the precursor as  $N_2O^{2+} \rightarrow N_2^+ + O^+ \rightarrow N^+ + O^+ + N$ .

The KER distribution for this channel is shown in Fig. 5. The KER values for this channel ( $3.6 \pm 0.4$ ,  $7.5 \pm 0.9$ , and  $13.4 \pm 3.0$  eV) above its thermodynamic threshold (39.6 eV) give the excited-state energies of  $N_2O^{2+}$  as  $43.2 \pm 0.4$ ,  $47.1 \pm 0.9$ , and  $53.0 \pm 3.0$ ; the former two values are in good agreement with the data of Love and Price [7].

(c)  $N^2 + N^+ + O$ ,  $N^{2+} + O^+ + N$ , and  $O^{2+} + N^+ + N$ . The weak structures for these islands can be identified in Fig. 1, but their analysis is not feasible due to the low counting statistics and the inseparability of the corresponding islands.

#### IV. CONCLUSIONS

The technique of coincident detection of momentum vectors of fragment ions of a precursor molecular ion is used to study the dissociative ionization of singly to triply ionized  $N_2O$  molecules in 10-keV electron interactions. The RIFs for the six observed coincidence channels are obtained and compared with a theoretical prediction and with the experimental data available for photon and ion impacts; the coincidence channel  $N^+ + NO^+$  is found to be the most dominant channel. Precursor-specific relative PICSSs for the six fragment ions are deduced from the experimental data and are used to establish that about 81.8% of single ionization, 17.8% of double ionization, and about 0.4% of triple ionization of the parent  $N_2O$  molecule contribute to the total fragment ion yield.

The kinetic energy release in various dissociation channels of  $N_2O^{2+}$  and  $N_2O^{3+}$  is studied. It is found that the CE model predicts higher values of KER as compared to that of the present experiment. For  $N^+ + NO^+$  and  $O^+ + N_2^+$  channels, most of the fragment ions are found to be formed in their respective ground electronic states if the vibrational excitation for diatomic fragments is considered. However, the possibility for a small contribution from indirect ionization

processes, especially in the case of  $N^+ + NO^+$ , also exists; the energy selected ejected-electron-fragment ion-coincident measurements can be fruitful for such identifications. The fragmentation channels involving a neutral atom are found to contribute significantly, in contrast to the earlier observations.

The mechanisms of dissociation for various fragmentation channels of the  $N_2O^{2+}$  and  $N_2O^{3+}$  precursor ions are discussed; it is suggested that a  $N^+ + O^+ + N$  channel is formed from sequential ( $N_2O^{2+} \rightarrow N_2^+ + O^+ \rightarrow N^+ + O^+ + N$ ) as well as from concerted decay of  $N_2O^{2+}$ . However, the  $N^+ + N^+ + O$  channel originates purely from the sequential decay process as  $N_2O^{2+} \rightarrow N^+ + NO^+ \rightarrow N^+ + N^+ + O$ .

The decay of  $N_2O^{3+}$  into  $N^+ + N^+ + O^+$  occurs purely via the concerted process with the central nitrogen ion being at rest, whereas the terminal nitrogen ion and the oxygen ion fly back to back.

#### ACKNOWLEDGMENTS

P.B., R.S., and N.Y. thankfully acknowledge partial supports by the Board of Research in Fusion Science & Technology (BRFST, Ahmedabad) and the Council of Scientific and Industrial Research (CSIR, New Delhi) during the progress of this work.

- 
- [1] D. Mathur, *Phys. Rep.* **391**, 1 (2004).
- [2] J. W. McConkey, C. P. Malone, P. V. Johnson, C. Winstead, V. McKoy, and I. Kanik, *Phys. Rep.* **466**, 1 (2008).
- [3] S. D. Price, *PhysChemChemPhys* **5**, 1717 (2003).
- [4] J. Ullrich, R. Moshhammer, R. Dörner, O. Jagutzki, V. Mergel, H. Schmidt-Böcking, and L. Spielberger, *J. Phys. B* **30**, 2917 (1997).
- [5] P. Forster *et al.*, in *Climate Change 2007: The Physical Science Basis*, edited by S. Solomon *et al.* (Cambridge University Press, New York, 2007).
- [6] [http://www.noaa.gov/stories/2009/20090827\\_ozone.html](http://www.noaa.gov/stories/2009/20090827_ozone.html).
- [7] N. A. Love and S. D. Price, *PhysChemChemPhys* **6**, 4558 (2004).
- [8] P. Bhatt, R. Singh, N. Yadav, and R. Shanker, *Phys. Rev. A* **85**, 034702 (2012).
- [9] S. D. Price, J. H. D. Eland, P. G. Fournier, J. Fournier, and P. Millie, *J. Chem. Phys.* **88**, 1511 (1988).
- [10] J. H. D. Eland and V. J. Murphy, *Rapid Commun. Mass Spectrom.* **5**, 221 (1991).
- [11] L. J. Frasinski, P. A. Hatherly, and C. Codling, *Phys. Lett. A* **156**, 227 (1991).
- [12] T. LeBrun, M. Lavollée, M. Simon, and P. Morin, *J. Chem. Phys.* **98**, 2534 (1993).
- [13] S. Hsieh and J. H. D. Eland, *J. Phys. B* **30**, 4515 (1997).
- [14] A. Hishikawa, A. Iwamae, K. Hoshina, M. Kono, and K. Yamanouchi, *Res. Chem. Intermed.* **24**, 765 (1998).
- [15] [www.gsi.de/annrep2002/files/90.pdf](http://www.gsi.de/annrep2002/files/90.pdf); [www.gsi.de/scirep2006/PAPERS/ATOMIC-PHYSICS-11.pdf](http://www.gsi.de/scirep2006/PAPERS/ATOMIC-PHYSICS-11.pdf).
- [16] M. Ueyama, H. Hasegawa, A. Hishikawa, and K. Yamanouchi, *J. Chem. Phys.* **123**, 154305 (2005).
- [17] M. Alagia, P. Candori, S. Falcinelli, M. Lavollée, F. Pirani, R. Richter, S. Stranges, and F. Vecchiocattivi, *Chem. Phys. Lett.* **432**, 398 (2006).
- [18] X. Zhou, P. Ranitovic, C. W. Hogle, J. H. D. Eland, H. C. Kapteyn, and M. M. Murnane, *Nature Phys.* **8**, 232 (2012).
- [19] N. Lévassieur and P. Millié, *J. Chem. Phys.* **92**, 2974 (1990).
- [20] R. Murphy and W. Eberhardt, *J. Chem. Phys.* **89**, 4054 (1988).
- [21] L. Ferrand-Tanaka, M. Simon, R. Thissen, M. Lavollée, and P. Morin, *Rev. Sci. Instrum.* **67**, 358 (1996).
- [22] R. Singh, P. Bhatt, N. Yadav, and R. Shanker, *Meas. Sci. Technol.* **22**, 055901 (2011).
- [23] P. Bhatt, R. Singh, N. Yadav, and R. Shanker, *Phys. Rev. A* **84**, 042701 (2011).
- [24] P. Bhatt, R. Singh, N. Yadav, and R. Shanker, *Phys. Rev. A* **85**, 042707 (2012).
- [25] W. C. Wiley and I. H. McLaren, *Rev. Sci. Instrum.* **26**, 1150 (1955).
- [26] M. R. Bruce, C. Ma, and R. A. Bonham, *Chem. Phys. Lett.* **190**, 285 (1992); M. R. Bruce, L. Mi, C. R. Sporleder, and R. A. Bonham, *J. Phys. B* **27**, 5773 (1994).
- [27] B. Siegmann, U. Werner, H. O. Lutz, and R. Mann, *J. Phys. B* **35**, 3755 (2002).
- [28] J. H. D. Eland, *Chem. Phys.* **294**, 171 (2003).